Estradiol accelerates endothelial healing through the retrograde commitment of uninjured endothelium.

Cédric Filipe, Lætitia Lam Shang Leen, Laurent Brouchet, Audrey Billon, Vincent Benouaich, Vincent Fontaine, Pierre Gourdy, Françoise Lenfant, Jean-François Arnal, Alain-Pierre Gadeau, et al.

Estradiol accelerates endothelial healing through the retrograde commitment of uninjured endothelium.

Running title: Estradiol action on reendothelialization

Cédric Filipe[1], Lætitia Lam Shang Leen[2], Laurent Brouchet[1], Audrey Billon[1], Vincent Benouaich[1], Vincent Fontaine[1], Pierre Gourdy[1], Françoise Lenfant[1], Jean-François Arnal[1], Alain-Pierre Gadeau[2], Henrik Laurell[1]

[1] INSERM U858, I2MR, équipe 9, Université de Toulouse III et CHU de Toulouse-Rangueil, BP 84225, 31432 Toulouse Cedex 4, FRANCE

[2] INSERM U828, Université de Bordeaux 2, 33600 Pessac, FRANCE

Correspondence to Henrik Laurell : laurell@toulouse.inserm.fr

Tel. +33 5 61 32 31 28

Fax. +33 5 61 32 21 41

The work was supported in part by Université Toulouse III and Faculté de Médecine de Toulouse-Rangueil, INSERM, the European Vascular Genomics Network No. 503254, Agence Nationale de la Recherche ANR-05-PCOD-011-01 “E2 and artery”, the Fondation de France, the Fondation de l'Avenir, and the Conseil Régional Midi-Pyrénées and Aquitaine in France.

Abbreviations: E2, 17ß-estradiol; EFCM, “en face” confocal microscopy; BrdU, 5-Bromo-2-deoxyuridine; REGEN, Regenerative area; RE, ReEndothelialized area; RetroP, Retrograde Proliferating zone;

Abstract

Although the accelerative effect of 17ß-estradiol (E2) on endothelial regrowth has been clearly demonstrated, the local cellular events accounting for this beneficial vascular action are still uncertain. In the present work, we compared the kinetics of endothelial healing of mouse carotid arteries after endovascular and perivascular injury. Both basal reendothelialization as well as the accelerative effect of E2 were similar in the two models. Three days after endothelial denudation, a “regenerative area” was observed in both models, characterized by similar changes in gene expression after injury, visualized by “en face” confocal microscopy (EFCM). A precise definition of the injury limits was only possible with the perivascular model, since it causes a complete and lasting decellularization of the media. Using this model, we demonstrated that migration of uninjured endothelial cells precedes proliferation (BrdU incorporation) and that these events occur at earlier time points with E2 treatment. We have also identified an uninjured retrograde zone as an intimate component of the endothelial regeneration process. Thus, in the perivascular model the "regenerative area" can be subdivided into a retrograde zone and a reendothelialized area. Importantly, both areas are significantly enlarged by E2.. In conclusion, the combination of the electric perivascular injury model and EFCM is well adapted to the visualization of the endothelial monolayer and to investigate cellular events involved in reendothelialization. This process is accelerated by E2 as a consequence of the retrograde commitment of an uninjured endothelial zone to migrate and proliferate contributing to an enlargement of the “regenerative area”.

Keywords : Endothelial regeneration, arterial injury, estrogen, carotid injury model, “en face” confocal microscopy

Introduction

The integrity and functionality of the arterial endothelium, the very thin cell monolayer positioned at the interface between the blood and the vessel wall, plays a crucial role in the physiology of circulation. Deendothelialization is the consequence of the treatment of coronary atherosclerosis disease by percutaneous transluminal coronary angioplasty, most often associated with intracoronary stents. One major drawback of this therapeutical approach is the residual in-stent restenosis, due to smooth muscle cell proliferation and intimal extracellular matrix accumulation. Drug-eluting stents releasing antimitotics (sirolimus, paclitaxel) efficiently prevent smooth muscle cell proliferation and thereby in-stent restenosis, but increase the risk of late stent thrombosis. This very serious event, commonly associated with sudden death or acute myocardial infarction, is at least partly the consequence of the inhibition of the reendothelialization of the stent struts by the antimitotics (13, 25).

The endothelial healing after injury process has previously mostly been studied in larger animals. More than 20 years ago, a series of pioneer studies unraveled several cellular mechanisms involved in endothelial regrowth after injury in rats and rabbits (19, 37, 38), refs in (42). To further gain insight in the molecular mechanisms, the possibility to use transgenic mice provides its obvious advantage. However, the endovascular injury model in mice, proposed by Lindner et al. (24) is laborious due to the very small size of the mouse carotid artery. As an alternative method, we more recently proposed a model of perivascular electric injury of the carotid artery (9), based on a femoral artery injury model developed by Carmeliet and colleagues (10). Even though the perivascular carotid model has been used in several published studies (8, 15, 41, 45), no systematic comparison with the endovascular injury has yet been reported, although both models behave similarly in terms of accelerated endothelial healing by 17β-estradiol (E2) estimated three days post injury by Evans blue staining (8).

Indeed, it is now clear that the physiological and pathophysiological role of E2 is not limited to reproductive organs, but involves many other tissues, in particular those belonging to the cardiovascular system. In particular, E2 exerts several beneficial effects at the level of the endothelium: it promotes endothelial NO production, prevents VCAM-1 expression and endothelial apoptosis (refs in (5, 28)). In

addition, E2 stimulates endothelial regrowth after endothelial denudation in rats (23) and in mice (9, 20, 40). Interestingly, inhibition of neointimal proliferation and acceleration of reendothelialization with the local administration of E2 following balloon angioplasty in a pig model has been recently reported (11, 30). Moreover, implantation of E2-eluting stents appears feasible and safe in humans (2).

E2 effects can be mediated by estrogen receptor alpha (ERα) and beta (ERβ), also named NR3A1 and NR3A2, referring to their classification within the nuclear receptor superfamily (1). The accelerative effect of E2 on reendothelialization is mediated by ERα (9) and endothelial NO synthase appears absolutely required for this effect (8, 20). Interestingly, the effect of E2 on endothelial healing remains unaltered upon inhibition of NO synthase activity by L-NAME (8). In addition, ERα also mediates the beneficial effect of E2 on medial hyperplasia (33). However, at least in mice, ERβ is not necessary for both these E2 effects on arterial healing (9, 22).

To further study the cellular mechanisms accounting for the accelerative effect of E2 on reendothelialization, we have compared the kinetics of reendothelialization in the conventional endovascular and a perivascular electric injury model using Evans blue staining. Since the endothelial cell monolayer is rather poorly visualized by immunohistochemical analyses on frozen transversal sections, we also applied « *en face*» confocal microscopy (EFCM) to more precisely visualize the regenerated endothelium, as well as the expression of several molecular key actors. We confirmed, in agreement with previous work in rat (38), the appearance of the "REGENerative area" (REGEN) characterized by endothelial cell proliferation and gene expression changes. At variance with the endovascular model, the injury limit can be precisely defined in the perivascular model by EFCM analysis. This feature revealed the implication of retrograde zone in the adjacent uninjured endothelium in the regenerative process. The commitment of this zone, named RetroP, could be of profound importance in the beneficial action of E2, as its size is increased upon E2 treatment.

Materials and methods

Mice

All procedures involving experimental animals were performed in accordance with the principles and guidelines established by the National Institute of Medical Research (INSERM). They were housed in cages in groups of 5, kept in a temperature-controlled facility on a 12-hour light-dark cycle, and fed normal laboratory mouse chow diet. At 4 weeks of age, C57BL/6J mice (Charles Rivers, L'arbresle, France) were ovariectomized, and pellets releasing either placebo or E2 (17β-estradiol 0.1mg, 60 days release, i.e. 80 µg/kg/d, Innovative Research of America, Sarasota, FL) were implanted subcutaneously in the back of the animals.

C57Bl/6-TgN(ACTbEGFP)1Osb transgenic mice (GFP-Tg, Jackson Laboratories, Bar Harbor, Maine) (31) with at least eight backcrosses with C57BL/6J mice, were used in bone marrow grafting experiments. Two weeks after ovariectomy**,** recipient C57Bl/6 mice were lethally irradiated (9Gy, γ-source) and received an intravenous injection of $4x10^6$ donor BM cells 24 h later. One month later, mice were implanted with either a placebo or an E2 pellet. Chimeric mice were sacrificed 3 days post-injury.
Mice were exposed to placebo or E2 for 2 weeks before artery injury and until sacrifice as previously described (9). We systematically checked that placebo-treated ovariectomized mice had an atrophied uterus (<20 mg) and non-detectable (<5pg/ml i.e. 20 x 10^{-12} M) circulating levels of E2, whereas those implanted with an E2 releasing pellet had a significant increase in uterine weight and serum E2 concentrations (100 to 150 pg/ml, not shown).

Mouse carotid injury

Endovascular injury was performed mechanically by a modification of the protocol described by Lindner and co-workers (24). Briefly, animals were anaesthetized by intraperitoneal injection of a mix of ketamine and xylasine (1% and 0.1% (w/v), respectively). The right common carotid artery was exposed from bifurcation, via an anterior incision of the neck. The left external carotid was ligated distally and looped proximally with 7-0 silk suture. Silk loops were placed around internal and common carotids to

temporally restrict blood flow in the area of surgical manipulation. The external carotid was incised. The injury was performed using a 0.3 mm diameter swab built by loosely winding and sticking an 8-0 silk suture around 0.16 mm diameter blunted guide wire. The swab was introduced, advanced through the common left carotid artery and withdrawn 3 times. A 4 mm length denudation from bifurcation of the common carotid artery was performed using the silk suture on the common carotid as injury. The device was removed and the external carotid ligated proximally. Blood flow was then restored in internal and common carotids. The skin incision was closed and animals were allowed to wake up under warm conditions.

The carotid electric injury was performed essentially as previously described (9). Briefly, the left common carotid artery was exposed as described above. The electric injury was applied to the distal part (4 mm precisely) of the common carotid artery with a bipolar microregulator.

One to 7 days later, the endothelial regeneration process was evaluated by staining the denuded areas with Evans blue dye as previously described (9). Briefly, 50 µL of solution containing 5% Evans blue diluted in saline was injected into the tail vein 10 minutes before euthanasia, followed by fixation with a perfusion of 4% phosphate-buffered formalin (pH 7.0) for 5 minutes. The left common carotid artery was dissected from the aortic arch to the carotid bifurcation. The artery was then opened longitudinally. The total and stained carotid artery areas were planimetered after image digitalization. The percentage of reendothelialization was calculated by $1-(A_{dayS}/A_{day0})* 100$, where A_{dayS} represents the remaining deendothelialized area at the day of sacrifice, and A_{day0} the initially deendothelialized area.

En face confocal microscopy

Intravascular blood was first removed with an intra cardiac injection of PBS 1X. The carotids were carefully dissected and fixed for 20 min in PBS containing 4% paraformaldehyde. Carotids were longitudinally opened and fixation was quenched with 100 mM glycine (pH 7.4), permeabilized for 10 min in 0.1% Triton X-100, and washed in PBS. Fixed tissues were blocked with a solution I (75 mM NaCl, 18mM Na_3citrate, 2% goat serum, 1% BSA, 0.05% Triton X-100, and 0.02% NaN_3) during 2h at room temperature. Primary antibody are diluted in solution I and incubated with carotids during 48h at

4°C. Then, tissues were washed with solution II (75 mM NaCl, 18 mM Na_3citrate, 0.05% Triton X-100) for 2h and rinsed in PBS. Carotids were incubated, 1h at room temperature, with fluorophore-conjugated antibodies (Molecular probes) diluted in solution I. Finally tissues were washed in solution I for 1h at room temperature. Primary antibodies used were: CD31 (01951D, Pharmingen), eNOS (sc654, Santa Cruz Biotechnologies), von Willebrand Factor (A0082, Dako). Secondary antibodies (Invitrogen) were all conjugated with Alexa Fluor 633. To label the nuclei, propidium iodide was used (Sigma-Aldrich). All preparations were mounted with Kaiser's glycerol gelatin (Merck). Microscopy imagery was performed on a LEICA SP2 confocal microscopy and quantification was performed with ZEISS LSM 510 software. Lengths of the reendothelialized area (RE) and of the retrograde proliferating zone (RetroP) are means of at least 10 measures spanning the carotid obtained with the software Zeiss LSM Image Browser v.3.1 (Carl Zeiss Jena Gmbh, Jena, Germany). The assembly of micrographs was achieved with PhotoStich v.3.1 (Canon, Courbevoie, France)

BrdU incorporation and staining

To label proliferating cells 3 or 5 days post-injury, the mice received an intraperitoneal injection of 100 µL 5-Bromo-2-deoxyuridine solution (33 mg/mL, Roche Diagnostic) 15 hours before sacrifice. At earlier time points (24, 36 or 50 h post-injury), the mice received an injection at time 0 and then approximately every 16 h. After tissue recovery, samples were fixed in 100% methanol during 30 min and permeabilized with 2N HCl during 7 min at 37°C. After 3 washes in PBS, samples were treated with a Borate solution (24.6 g/L $Na_2B_4O_7$, 4.36 g/L KH_2PO_4) during 15 min. Carotid arteries were subsequently incubated with solution I (previously described) for 2 hours at RT. Finally, tissues were incubated with anti-BrdU antibody conjugated with Alexa fluor 633 (Invitrogen) during 1 hour at RT and rinsed in solution II (described above). A mean length of each zone (REGEN, RE, RetroP) was measured was obtained as described above.

Statistics

Results are expressed as means ±S.E.M. To test the role of E2 treatment on reendothelialization, a one-factor ANOVA was performed. To test the respective role of E2 treatment and type of injury or time on reendothelialization, a two-factor ANOVA was performed. When an interaction was observed between the two factors, the four groups were compared by a one-factor ANOVA. $P<0.05$ was considered as statistically significant.

Results

Endovascular and perivascular electric injury models exhibit similar kinetics of both basal and E2 stimulated reendothelialization

In order to compare the reendothelialization process after endovascular and perivascular electric carotid injury, we performed an injury of equal length (4 mm) in both models in ovariectomized mice treated with either placebo or E2. Under these conditions the reendothelialization is completed seven days after both types of injury (data not shown), as previously observed (9). Therefore, the kinetics of reendothelialization was analyzed at 3 and 5 days post-injury. Interestingly, no difference in the kinetics of the endothelial healing was observed between both models (Figure 1). To test the respective role of injury type and E2 treatment on reendothelialization at each time point, a two-factor ANOVA was performed and revealed a significant effect of E2 on acceleration of reendothelialization at day 3 and day 5 (both $P<0.05$), but no effect of the type of injury and no interaction between the two parameters. Thus, no difference in the rate of the endothelial healing could be detected between both models.

"En face" confocal immunohistochemical analysis of endovascular and perivascular electric carotid injury reveals similarities between the two models in terms of reendothelialization

We next wanted to gain further insight in molecular and cellular events during reendothelialization in both injury models at 3 days post injury. Since the visualization of the endothelial cell monolayer by transversal sections is limited, we employed EFCM on longitudinally opened and flattened mouse carotid arteries. As the endothelial regeneration in both models progresses mainly from the proximal edge of the lesion, in the direction of the blood flow, we focused on this region for further studies. Staining by propidium iodide confirmed that the endothelial and smooth muscle cell nuclei could be distinguished by their orientation, size and shape. Indeed, in contrast to smooth muscle, endothelial cell nuclei were oriented in the direction of the blood flow, and were larger and rounder in shape than smooth muscle cell nuclei. Compared to the intact endothelium, EFCM analysis revealed a decreased expression of von

Willebrand factor (vWF) and PECAM (CD31), and an increased expression of eNOS in the injured area, irrespective of the injury model (Figures 2A-C, 2A'-C').

We then determined the proliferative index of the endothelial cells following a peritoneal injection of BrdU, 15 hours prior to sacrifice. The fraction of BrdU positive cells after endovascular injury (38.6 ± 4.6%) and perivascular injury (44.3 ± 3.9%) did not differ significantly (P=0.35) (Figures 2D and 2D').

In agreement with previous reports (24), endovascular carotid injury using a thin swab preserves most of the vascular smooth muscle cells (Figure 2E). In contrast, perivascular electric carotid injury provokes a complete decellularization of both the intima and the media (Figure 2E'), without any cellular recolonization of the latter one week after injury. Thus, at variance with the endovascular model, the electric model permits the precise definition of the injury limit using EFCM.

Electric injury model analyzed by EFCM also allowed to determine two distinct areas: the "ReEndothelialized area" (RE) corresponding to the part of the injured intima that has been recolonized with endothelial cells and the "REGENerative area" (REGEN), corresponding to the zone of proliferating cells. In these ovariectomized mice, the REGEN was only slightly larger than the RE. Interestingly, the overexpression of eNOS and the lowered expression of vWF and CD31 were overlapping with the REGEN both in the endovascular (Figures 2A-D) and in the perivascular (Figures 2A'-D') model.

Taken together, we show here that even though the media exhibits major differences in the two injury models, the endothelial cells of the REGEN had similar characteristics in both models. Since both injury models exhibited similar kinetics of reendothelialization (Figure 1), but only the electric model in combination with EFCM allowed a precise localization of the injury limit due to the absence of cellular recolonization of the media (Figure 2E'), this latter model was chosen for most of the subsequent experiments.

"En face" confocal immunohistochemical analysis of perivascular electric carotid injury reveals the absence of medial smooth muscle regeneration within in the first week post-injury.

One of the surprising features of the model of perivascular electric carotid injury was the total absence of regeneration of the media at day 7, at a time when the reendothelialization was completed. We therefore decided to explore the regeneration of the medial layer at day 1, 3 and 5 post-injury. We first observed that, at these different time point, the limit of injury remained abrupt, with no visible evidence of migrating cells and with no change in smooth muscle cell density (Fig 2E'). Second, we determined the proliferative index of the smooth muscle cells following a peritoneal injection of BrdU, 15 hours prior to sacrifice. The fraction of BrdU positive cells was always < 1% of the cells examined at the edge of the injury, i.e. less than one medial cell per carotid artery examined (not shown). Third, the "en face" technique also offers the opportunity to precisely determine the abundance of bone-marrow derived cells in hematopoietic chimeric GFP mice (bone marrow from GFP transgenic mice grafted to irradiated wild type mice). However, whereas the number of GFP positive cells in the REGEN was about 4% and were very abundant in the adventitia, no GFP positive cells could be detected in the media ((14) and not shown).

Analysis by EFCM of E2-stimulated reendothelialization at day 3 after perivascular injury reveals the commitment of a retrograde zone.

E2 treatment elicited two main modifications at day 3 post-injury. First, EFCM confirmed that E2 accelerates the reendothelialization process (Figures 3 and 4), in agreement with data obtained through Evans blue staining (Figure 1). Second, E2 induces the enlargement of REGEN in the adjacent uninjured area (Figure 3B). BrdU labeling enabled the visualization of this "Retrograde Proliferating zone" (RetroP), defined as the area with a density ≥10% of BrdU positive cells. RetroP was present in placebo-treated mice, but was impressively increased by E2 (Figure 3B and 4). Changes in expression levels, such as increased eNOS, decreased CD31 and vWF, observed in RE also overlapped with RetroP (Figures 3B and C).

The quantification showed that E2 increased RE by 32.9%, and REGEN by 43.5%, both $P<0.05$ (Figure 4A). Moreover, the combination of EFCM and BrdU labeling allowed us to define the proliferation index as well as the total number of endothelial cells. Compared to placebo, E2 increased in

the RE the total number of BrdU-positive cells by 93.4 % and the total cell number by 86.1 %, both $P<0.05$ (Figure 4B and 4C). As the density of BrdU-positive cells in RE was not significantly increased by E2, the increase in total number of BrdU-positive cells was mainly due to the increased size of RE. The proliferative effect of E2 was even more spectacular in the RetroP. Indeed, E2 not only increased the size of RetroP (from 75±7 µm to 163±29 µm, $P<0.05$), but also the percentage of BrdU-positive cells in this zone (from 16.0 ± 1.3 to 42.4 ± 1.2%, $P<0.05$), this latter value being similar to that found in the RE. Altogether, E2 drastically (10-fold) increased the total number of BrdU-positive cells in the RetroP (Figure 4C).

In the endovascular injury model 3 days post injury, where only REGEN could be defined due to the lack of a precise determination of the injury limit, E2 increased the REGEN (+37.4%, $P<0.05$) to a similar extent as in the perivascular injury model (not shown). Indeed, a two-way ANOVA did not reveal any interaction between the E2 effect and the model used. Furthermore, the percentage of BrdU-positive cells in REGEN was very similar in E2 and placebo-treated mice (35.7 ± 3.2% and 36.0 ± 2.1% respectively, $P=0.87$, not shown), which is very close to the observations made in the perivascular injury model.

Early events in reendothelialization: endothelial migration precedes proliferation - effect of E2

To characterize the initial cellular responses in endothelial regrowth with respect to cell migration and proliferation, we used the perivascular model followed by repeated intraperitoneal administrations of BrdU on average every 16h. At 24 h post-injury, neither endothelial cell migration nor cell proliferation was observed in both E2- and placebo-treated mice (data not shown).

At 36 h after injury, the front of endothelial cells had clearly started to colonize the injured area, and the reendothelialized surface was significantly increased by E2 (+50.4%, $P<0.05$) (Figure 5A and 5B). However, as for the observation at 24 h, no BrdU labeled cells were detected in any condition at 36 h post injury (Figure 5A). When the same analysis was performed 50 h post injury, cellular proliferation was observed in half (3/6) of the E2-treated mice, but never (0/6) in placebo-treated mice (Figure 5C). Of note,

in BrdU positive E2 treated carotids, the percentage of labeled cells (39.2±5.0%) was already close to that observed at day 3 or day 5, indicating that the onset of proliferation quickly reached its maximal level.

The results shown in figures 5A and 5B clearly showed that migration of endothelial cells precedes the proliferative response, and that both of these processes appeared earlier under E2 treatment. The fact that the RE at 36h was larger in E2-treated mice than in control mice in the absence of proliferation could be explained by several mechanisms. One possibility is that an equal number of cells had migrated into the injured area in both placebo and E2 treated mice, but that the cells in the latter group had an increased size and therefore covered a larger surface. To test this hypothesis, the cellular density in RE was measured by counting of propidium iodide stained nuclei in the intima of carotids 36h and 50h post-injury. Since we did not observe any significant difference in cellular density in the two conditions, this would imply that more cells are recruited in the healing process under E2 treatment. These cells could either derive from circulating cells and/or from increased migration of surrounding uninjured endothelial cells. In order to determine whether the recruitment and incorporation of bone-marrow derived cells could account for the observed difference, we performed transplantation of GFP-positive bone-marrow into wild type mice. The “en face” confocal microscopy technique offers the opportunity to precisely determine the percentage of bone-marrow derived cells at different levels in the artery wall. Unexpectedly, E2 did not increase the density of GFP positive cells in the RE (3.4±1.2%,) compared to placebo (4.2±0.9%), NS (data not shown), although it increased the total number of GFP positive cells in the REGEN in proportion to the increase in its size, as previously reported (20, 40).

However, we found that E2 engages the migration of more endothelial cells from the uninjured area into the injured area. Indeed, as shown in figure 5C, depicting data from carotids 50 hours post injury, E2 decreased the cell density further upstream the injury limit (in the retrograde uninjured endothelium) than did the placebo. Noteworthy, the decrease in the cell number in this region coincided with the increase in cells observed downstream the injury limit (in the RE) in E2-treated mice. Thus, E2 mobilized a larger retrograde area and thereby a larger number of endothelial cells to migrate.

Taken together, these results demonstrate that endothelial cell migration constitutes an early cellular response to injury which precedes endothelial proliferation, and that E2 generated an earlier and

enhanced action of both of these processes through the recruitment of a larger area of uninjured endothelium. As the surface of uninjured "committed" endothelium, with decreased cellular density, was considerably larger than the retrograde proliferating zone (RetroP) at both day 2 (figure 5C) and at day 3 (not shown), we next sought to examine the evolution of RetroP at a later time point.

Accentuation of the retrograde proliferation at day 5 post injury in Placebo- and E2-treated mice.

The size of RetroP at day 5 was significantly larger than at day 3 both in placebo and E2 treated mice (Figure 6) and corresponded well with the size of the "committed zone", exhibiting a decreased cell density at day 3 (not shown). The size of both RE and RetroP in both placebo and E2 treated mice increased progressively and significantly from day 2 to day 3 and from day 3 to day 5 ($P<0.05$)(Figure 6B). Moreover, both RE and RetroP were significantly larger under E2 treatment compared to placebo at all time points (Figure 6B).

These analyses by EFCM confirmed the effect of E2 on reendothelialization obtained by Evans blue staining (Figure 1). At Day 30, when reendothelialization was completed for about 3 weeks, no proliferation was observed in both placebo- and E2-treated mice (not shown).

In summary, these data suggest that the decreased endothelial cell density observed in the retrograde uninjured endothelium at earlier time points give rises to a subsequent proliferative response covering a similar surface. E2 not only increased the RE corresponding to the previously reported acceleration of reendothelialization, but it clearly promoted the progressive recruitment of a retrograde zone in the adjacent uninjured endothelium (RetroP) which substantially contributed to the regenerative capacity of the REGEN.

E2 does not alter medial smooth muscle regeneration

We also explored the regeneration of the medial layer at day 1, 3 and 5 post-injury in response to E2. As in placebo-treated mice, the limit of injury remained abrupt, with no visible migrating cells and with no change in smooth muscle cell density, < 1% of proliferating smooth muscle cells, and no GFP positive cells could be detected in the injured media at variance with the intima and adventitia (not

shown). Altogether, these data confirm that the limit of injury can be reliably defined by the front of the smooth muscle cells.

Discussion

The main achievements of the present study are:

(i) The conventional endovascular and the perivascular electric injury model were found to be undistinguishable in terms of basal and E2-elicited reendothelialization.

(ii) A "REGENerative area" characterized by endothelial cell proliferation and gene expression changes is similar in both of the mouse models, and E2 elicit an enlargement of this REGEN.

(iii) In contrast to the endovascular model, the underlying smooth muscle cells are destroyed in the injured area of the perivascular electric model, and do not regenerate during the first week, allowing to precisely define the injury limit. This permitted to subdivide REGEN into a reendothelialized area (RE, in the uninjured area) and a retrograde proliferating zone (RetroP, in the adjacent uninjured endothelium).

(iv) E2 strongly increased the retrograde commitment of adjacent uninjured endothelium, which is first distinguished by the mobilization of endothelial cells and a decrease in cellular density, followed by a proliferative response. This increase of RetroP, in addition to the increase of RE, contributed to the enlargement of the "regenerative area", which are likely to represent key events in the acceleration of reendothelialization.

(i) Endovascular and electric perivascular injuries can be similar in their efficiency to destroy the endothelium, but they differ significantly in their effects on the underlying cell populations in the vessel wall. Endovascular injury preserves most of the adventitial cells as well as most of the medial smooth muscle cells (24). In both models the intima is regenerated after one week, however in the perivascular model, the media does not show any sign of regeneration during the time of reendothelialization. As both models had similar characteristics with respect to basal and E2-elicited reendothelialization (evaluated by Evans Blue staining), changes in gene expression and proliferative response (see below), this would suggest a minor, if any, role of the smooth muscle cells in the injured area in the reendothelialization process. However, smooth muscle cells in the RetroP area might play an important role (see below). The perivascular model offers various major advantages, such as no modification of the flow in the carotid

artery associated to the ligature of external carotid artery, rapidity and reliability (thrombosis rate 5-10% versus 30% in the endovascular). Moreover, perivascular electric injury can be easily transferred from one experimenter to another and requires less operator skill than the endovascular injury. Taken together, all these similarities allowed us to conclude that perivascular electric injury represents a valid and alternative model to endovascular injury.

(ii) More than two decades ago several researchers, as Reidy, Clowes, Schwartz, and others (12, 19, 37-39) beautifully described different cellular events involved in reendothelialization models of endovascular artery injury in the rat or the rabbit. In concordance with our data, Schwartz and colleagues showed that proliferation (using 3H-thymidine incorporation) of endothelial cells from each side of the adjacent uninjured area was not restricted to the front edge, but involved up to 100 rows of endothelial cells, contributing to a "regeneration zone" (38). Using BrdU incorporation, we observed here in mouse a similar "regenerative area" (REGEN). At variance with the study by Schwartz et al., we did not observe any proliferating cells 24h or even 36 h post-injury. It is possible that this divergence could in part be due to differences between blood vessels (carotid versus aorta) or species (mouse versus rat). Species-dependent differences in regenerative capacity have indeed been reported. The endothelium of the rabbit carotid is, for instance, less prone to heal than that of rats (36)

Not surprisingly, we observed that the regenerative process was also characterized by marked alterations of gene expression. It is of interest to note that these changes appear over the entire REGEN including both injured and uninjured areas. Increased eNOS expression was reported 10 years ago by Berk and coworkers in the regenerative area after rat carotid injury (34). The expression of eNOS is also increased in proliferating cultured endothelial cells (6). More recently, Losordo and colleagues demonstrated that the eNOS is also indispensable in the accelerative effect of E2 on reendothelialization (20) even though it is independent of the NO producing activity of eNOS (8).

(iii) We also explored the regeneration of the smooth muscle cells in the injured media in the perivascular electric model. Surprisingly, at variance to the rapid endothelial healing, we could not detect

any significant features of migration or proliferation of the adjacent uninjured smooth muscle cells during the first week, neither infiltration of bone marrow-derived cells in the media. We can not provide an explanation for the absence of rapid regeneration of the media. The high expression of eNOS in the regenerated endothelium could be one contributing factor, as elevated eNOS levels are known to inhibit smooth muscle cell proliferation and migration (21, 43). The absence of the underlying smooth muscle cells and the lack of their regeneration (at least during the first week) have two major consequences. First, only the electric injury model allows to precisely define the limit of the injury, and thereby to further divide REGEN into a reendothelialized area (RE) and a "retrograde proliferating zone" (RetroP). Second, it suggests, given the similarities between the results observed in the two models of reendothelialization, that the underlying smooth muscle cells in the injured area do not appear to be of importance in endothelial healing. However, it does not rule out that those in the RetroP could still play an important role. The suggested lack of role of the smooth muscle cells in the injured zone for both basal and estradiol-induced reendothelialization (Figure 1) should not be interpreted as a general conclusion concerning the mechanisms involved in other treatments that influence the kinetics of endothelial healing.

(iv) At day 3 post-injury, the enlargement of REGEN by E2 (Figure 4A) was the outcome of an increased surface of both the RE and the RetroP, a zone expanding the REGEN into the adjacent uninjured area. E2 treatment did not alter the percentage of the BrdU-positive cells in the RE, but increased this percentage in the RetroP to a level similar to that observed in the RE (Figure 4B). Thus, E2 recruited cells to proliferate mainly by increasing in the size of the proliferative cell area (REGEN = RE + RetroP). These phenomena were magnified at day 5 post injury, in particular the effect of E2 on RetroP (Figure 6). Earlier time points revealed that E2 initially accelerated cell migration, leading to a decrease in cellular density in the upstream uninjured endothelium over a distance that was 3-fold longer under E2 (Figure 5C). This is likely to be directly contributing factor to the increased size of RetroP, defined by proliferating cells, observed after E2 treatment (Figure 6). Thus, the spatio-temporal "commitment" of the adjacent uninjured endothelium occured earlier under E2, leading to a larger and precocious RetroP, which could represent a key event in reendothelialization and the emergence of REGEN.

Whereas E2 is known to promote endothelial cell migration and proliferation *in vitro* (17, 18, 29), the present study is, to our knowledge, the first demonstration of a clear distinction between E2-stimulated migration and proliferation of endothelial cells *in vivo*. It was initially believed that E2 accelerated reendothelialization mainly through a local effect on adjacent residing uninjured endothelium. However, several studies have shown that arterial healing can be significantly modulated by circulating bone marrow (BM)-derived cells as monocyte-macrophages (16), platelets (27) or endothelial progenitor cells (EPCs) (4, 7, 35). E2 increases the number of circulating EPCs as well as the incorporation of BM-derived cells in the reendothelialized area (20, 40). However, the present work does not suggest that the incorporation of these BM-derived cells substantially contribute in the endothelial regeneration process, as the percentage of GFP positive cells was low (about 4%) and did not differ in E2 or placebo treated mice. We can not exclude a potential role of non-BM derived progenitor cells, since homing of these cells seems important in neovascularization after hind leg ischemia (3). Third, platelets are abundant in the deendothelialized area (9, 26) and release factors that can directly (32) or indirectly (27) contribute to accelerate reendothelialization. Indeed, we previously reported that BM FGF2 is absolutely required in the accelerative effect of E2 in reendothelialization, whereas extra-BM FGF2 is dispensable (14), suggesting that FGF2 is a key mediator of the E2 action at the level of the BM. The "en face" analysis by EFCM, does not suggest that BM-derived cells contribute substantially as "cobble stones" of the regenerated endothelial "pavement", at least not in the repair process in the models used in the present study, in which the injury is limited to 4 mm and reendothelialization completed after one week. This does not exclude that the incorporation of BM-derived progenitor cells in the intima could be of importance in the repair of arterial injuries spanning larger surfaces for which healing takes several weeks or even stays incomplete. Nonetheless, despite the scarcity of these cells, they could play an important role through a paracrine action. The identification of the specific BM-derived cell populations responsible for the reendothelialization process will require the development of the cell-specific inactivation of ERα in these BM-derived populations, tools that are not yet available.

In conclusion, we demonstrate here that E2 stimulates the retrograde commitment of an uninjured endothelial zone to proliferate (RetroP), contributing to an enlargement of the "REGENerative area" and to an acceleration of reendothelialization. A similar scenario ought henceforth to be considered in other situations of accelerated reendothelialization (eg. by statins) (44). We believe that the perivascular electric injury coupled with "en face" confocal microscopy (EFCM) will represent a powerful model to further investigate the cellular mechanisms underlying the reendothelialization process. A better understanding of the mechanisms of artery healing will help to propose new strategies to optimize post-angioplasty and in-stent reendothelialization. An enlargement of the "regenerative area" and the "commitment" of surrounding uninjured tissue, endothelial or not, ought also to be considered in other healing processes.

Acknowledgments:

The work was supported in part by Université Toulouse III and Faculté de Médecine de Toulouse-Rangueil, INSERM, the European Vascular Genomics Network No. 503254, Agence Nationale de la Recherche ANR-05-PCOD-011-01 “E2 and artery”, the Fondation de France, the Fondation de l'Avenir, and the Conseil Régional Midi-Pyrénées and Aquitaine in France. We thank Cochard P., Jauneau A., Martinez Y and. Knibiehler B for the support and analysis of confocal data, Barreira Y. at the I2MR animal facility, Bayard F. for fruitful discussions and Fouque M.J. for excellent technical assistance.

C.F. was supported by a grant from the Groupe de Réflexion et de Recherche Cardiovasculaire and V.F. was supported by a grant from the Nouvelle Société Française d’Athérosclérose.

References:

1. A unified nomenclature system for the nuclear receptor superfamily. *Cell* 97: 161-163, 1999.
2. **Abizaid A, Albertal M, Costa MA, Abizaid AS, Staico R, Feres F, Mattos LA, Sousa AG, Moses J, Kipshidize N, Roubin GS, Mehran R, New G, Leon MB, and Sousa JE.** First human experience with the 17-beta-estradiol-eluting stent: the Estrogen And Stents To Eliminate Restenosis (EASTER) trial. *J Am Coll Cardiol* 43: 1118-1121, 2004.
3. **Aicher A, Rentsch M, Sasaki K, Ellwart JW, Fandrich F, Siebert R, Cooke JP, Dimmeler S, and Heeschen C.** Nonbone marrow-derived circulating progenitor cells contribute to postnatal neovascularization following tissue ischemia. *Circ Res* 100: 581-589, 2007.
4. **Aicher A, Zeiher AM, and Dimmeler S.** Mobilizing endothelial progenitor cells. *Hypertension* 45: 321-325, 2005.
5. **Arnal JF, Scarabin PY, Tremollieres F, Laurell H, and Gourdy P.** Estrogens in vascular biology and disease: where do we stand today? *Curr Opin Lipidol* 18: 554-560, 2007.
6. **Arnal JF, Yamin J, Dockery S, and Harrison DG.** Regulation of endothelial nitric oxide synthase mRNA, protein, and activity during cell growth. *Am J Physiol* 267: C1381-1388, 1994.
7. **Asahara T and Kawamoto A.** Endothelial progenitor cells for postnatal vasculogenesis. *Am J Physiol Cell Physiol* 287: C572-579, 2004.
8. **Billon A, Lehoux S, Lam Shang Leen L, Laurell H, Filipe C, Benouaich V, Brouchet L, Dessy C, Gourdy P, Gadeau AP, Tedgui A, Balligand JL, and Arnal JF.** The estrogen effects on endothelial repair and mitogen-activated protein kinase activation are abolished in endothelial NO synthase knockout mice, but not by NO synthase inhibition by N-nitro-L-arginine methyl ester (L-NAME). *Am J Pathol* (in press), 2008.
9. **Brouchet L, Krust A, Dupont S, Chambon P, Bayard F, and Arnal JF.** Estradiol accelerates reendothelialization in mouse carotid artery through estrogen receptor-alpha but not estrogen receptor-beta. *Circulation* 103: 423-428., 2001.
10. **Carmeliet P, Moos L, Stassen J, De Mol M, Bouché A, van den Oord J, Kocks M, and Collen D.** Vascular wound healing and neointima formation induced by perivascular electric injury in mice. *Am J Pathol* 150: 761-776, 1997.
11. **Chandrasekar B and Tanguay JF.** Local delivery of 17-beta-estradiol decreases neointimal hyperplasia after coronary angioplasty in a porcine model. *J Am Coll Cardiol* 36: 1972-1978, 2000.
12. **Clowes AW, Clowes MM, and Reidy MA.** Kinetics of cellular proliferation after arterial injury. III. Endothelial and smooth muscle growth in chronically denuded vessels. *Lab Invest* 54: 295-303, 1986.

13. **Farb A and Boam AB.** Stent Thrombosis redux--the FDA Perspective. *N Engl J Med* 356: 984-987, 2007.

14. **Fontaine V, Filipe C, Werner N, Gourdy P, Billon A, Brouchet L, Garmy-Susini B, Bayard F, Prats H, Doetschman T, Nickenig G, and Arnal J.** Essential role of medullar FGF2 in the effect of estradiol on reendothelialization and EPCs mobilization. *Am J Pathol* 169: 1855–1862, 2006.

15. **Fontaine V, Filipe C, Werner N, Gourdy P, Billon A, Garmy-Susini B, Brouchet L, Bayard F, Prats H, Doetschman T, Nickenig G, and Arnal JF.** Essential role of bone marrow fibroblast growth factor-2 in the effect of estradiol on reendothelialization and endothelial progenitor cell mobilization. *Am J Pathol* 169: 1855-1862, 2006.

16. **Fujiyama S, Amano K, Uehira K, Yoshida M, Nishiwaki Y, Nozawa Y, Jin D, Takai S, Miyazaki M, Egashira K, Imada T, Iwasaka T, and Matsubara H.** Bone marrow monocyte lineage cells adhere on injured endothelium in a monocyte chemoattractant protein-1-dependent manner and accelerate reendothelialization as endothelial progenitor cells. *Circ Res* 93: 980-989, 2003.

17. **Geraldes P, Sirois MG, Bernatchez PN, and Tanguay JF.** Estrogen regulation of endothelial and smooth muscle cell migration and proliferation: role of p38 and p42/44 mitogen-activated protein kinase. *Arterioscler Thromb Vasc Biol* 22: 1585-1590, 2002.

18. **Geraldes P, Sirois MG, and Tanguay JF.** Specific contribution of estrogen receptors on mitogen-activated protein kinase pathways and vascular cell activation. *Circ Res* 93: 399-405, 2003.

19. **Haudenschild CC and Schwartz SM.** Endothelial regeneration. II. Restitution of endothelial continuity. *Lab Invest* 41: 407-418, 1979.

20. **Iwakura A, Luedemann C, Shastry S, Hanley A, Kearney M, Aikawa R, Isner JM, Asahara T, and Losordo DW.** Estrogen-mediated, endothelial nitric oxide synthase-dependent mobilization of bone marrow-derived endothelial progenitor cells contributes to reendothelialization after arterial injury. *Circulation* 108: 3115-3121, 2003.

21. **Janssens S, Flaherty D, Nong Z, Varenne O, van Pelt N, Haustermans C, Zoldhelyi P, Gerard R, and Collen D.** Human endothelial nitric oxide synthase gene transfer inhibits vascular smooth muscle cell proliferation and neointima formation after balloon injury in rats. *Circulation* 97: 1274-1281, 1998.

22. **Karas RH, Hodgin JB, Kwoun M, Krege JH, Aronovitz M, Mackey W, Gustafsson JA, Korach KS, Smithies O, and Mendelsohn ME.** Estrogen inhibits the vascular injury response in estrogen receptor beta-deficient female mice. *Proc Natl Acad Sci U S A* 96: 15133-15136, 1999.

23. **Krasinski K, Spyridopoulos I, Asahara T, van der Zee R, Isner JM, and Losordo DW.** Estradiol accelerates functional endothelial recovery after arterial injury. *Circulation* 95: 1768-1772, 1997.

24. **Lindner V, Fingerle J, and Reidy MA.** Mouse model of arterial injury. *Circ Res* 73: 792-796, 1993.

25. **Luscher TF, Steffel J, Eberli FR, Joner M, Nakazawa G, Tanner FC, and Virmani R.** Drug-eluting stent and coronary thrombosis: biological mechanisms and clinical implications. *Circulation* 115: 1051-1058, 2007.

26. **Massberg S, Gawaz M, Gruner S, Schulte V, Konrad I, Zohlnhofer D, Heinzmann U, and Nieswandt B.** A crucial role of glycoprotein VI for platelet recruitment to the injured arterial wall in vivo. *J Exp Med* 197: 41-49, 2003.

27. **Massberg S, Konrad I, Schurzinger K, Lorenz M, Schneider S, Zohlnhoefer D, Hoppe K, Schiemann M, Kennerknecht E, Sauer S, Schulz C, Kerstan S, Rudelius M, Seidl S, Sorge F, Langer H, Peluso M, Goyal P, Vestweber D, Emambokus NR, Busch DH, Frampton J, and Gawaz M.** Platelets secrete stromal cell-derived factor 1alpha and recruit bone marrow-derived progenitor cells to arterial thrombi in vivo. *J Exp Med* 203: 1221-1233, 2006.

28. **Mendelsohn ME and Karas RH.** Molecular and cellular basis of cardiovascular gender differences. *Science* 308: 1583-1587, 2005.

29. **Morales DE, McGowan KA, Grant DS, Maheshwari S, Bhartiya D, Cid MC, Kleinman HK, and Schnaper HW.** Estrogen promotes angiogenic activity in human umbilical vein endothelial cells in vitro and in a murine model. *Circulation* 91: 755-763, 1995.

30. **New G, Moses JW, Roubin GS, Leon MB, Colombo A, Iyer SS, Tio FO, Mehran R, and Kipshidze N.** Estrogen-eluting, phosphorylcholine-coated stent implantation is associated with reduced neointimal formation but no delay in vascular repair in a porcine coronary model. *Catheter Cardiovasc Interv* 57: 266-271, 2002.

31. **Okabe M, Ikawa M, Kominami K, Nakanishi T, and Nishimune Y.** 'Green mice' as a source of ubiquitous green cells. *FEBS Lett* 407: 313-319, 1997.

32. **Pakala R, Willerson JT, and Benedict CR.** Mitogenic effect of serotonin on vascular endothelial cells. *Circulation* 90: 1919-1926, 1994.

33. **Pare G, Krust A, Karas RH, Dupont S, Aronovitz M, Chambon P, and Mendelsohn ME.** Estrogen receptor-alpha mediates the protective effects of estrogen against vascular injury. *Circ Res* 90: 1087-1092, 2002.

34. **Poppa V, Miyashiro JK, Corson MA, and Berk BC.** Endothelial NO synthase is increased in regenerating endothelium after denuding injury of the rat aorta. *Arterioscler Thromb Vasc Biol* 18: 1312-1321, 1998.

35. **Rafii S and Lyden D.** Therapeutic stem and progenitor cell transplantation for organ vascularization and regeneration. *Nat Med* 9: 702-712, 2003.

36. **Reidy MA, Clowes AW, and Schwartz SM.** Endothelial regeneration. V. Inhibition of endothelial regrowth in arteries of rat and rabbit. *Lab Invest* 49: 569-575, 1983.

37. **Reidy MA and Schwartz SM.** Endothelial regeneration. III. Time course of intimal changes after small defined injury to rat aortic endothelium. *Lab Invest* 44: 301-308, 1981.

38. **Schwartz SM, Haudenschild CC, and Eddy EM.** Endothelial regeneration. I. Quantitative analysis of initial stages of endothelial regeneration in rat aortic intima. *Lab Invest* 38: 568-580, 1978.

39. **Spagnoli LG, Pietra GG, Villaschi S, and Johns LW.** Morphometric analysis of gap junctions in regenerating arterial endothelium. *Lab Invest* 46: 139-148, 1982.

40. **Strehlow K, Werner N, Berweiler J, Link A, Dirnagl U, Priller J, Laufs K, Ghaeni L, Milosevic M, Bohm M, and Nickenig G.** Estrogen increases bone marrow-derived endothelial progenitor cell production and diminishes neointima formation. *Circulation* 107: 3059-3065, 2003.

41. **Umetani M, Domoto H, Gormley AK, Yuhanna IS, Cummins CL, Javitt NB, Korach KS, Shaul PW, and Mangelsdorf DJ.** 27-Hydroxycholesterol is an endogenous SERM that inhibits the cardiovascular effects of estrogen. *Nat Med* 13: 1185-1192, 2007.

42. **Van Belle E, Bauters C, Asahara T, and Isner JM.** Endothelial regrowth after arterial injury: from vascular repair to therapeutics. *Cardiovasc Res* 38: 54-68, 1998.

43. **von der Leyen HE, Gibbons GH, Morishita R, Lewis NP, Zhang L, Nakajima M, Kaneda Y, Cooke JP, and Dzau VJ.** Gene therapy inhibiting neointimal vascular lesion: in vivo transfer of endothelial cell nitric oxide synthase gene. *Proc Natl Acad Sci U S A* 92: 1137-1141, 1995.

44. **Walter DH, Rittig K, Bahlmann FH, Kirchmair R, Silver M, Murayama T, Nishimura H, Losordo DW, Asahara T, and Isner JM.** Statin therapy accelerates reendothelialization: a novel effect involving mobilization and incorporation of bone marrow-derived endothelial progenitor cells. *Circulation* 105: 3017-3024, 2002.

45. **Zhu W, Saddar S, Seetharam D, Chambliss KL, Longoria C, Silver DL, Yuhanna IS, Shaul PW, and Mineo C.** The Scavenger Receptor Class B Type I Adaptor Protein PDZK1 Maintains Endothelial Monolayer Integrity. *Circ Res*, 2008.

Figure legends

Figure 1. Effect of estradiol (E2) on the reendothelialization process evaluated by Evans blue staining 3 and 5 days after endovascular or perivascular injury.

The percentage of reendothelialization was calculated by $1-(A_{dayS}/A_{day0})* 100$, where A_{dayS} represents the remaining deendothelialized area at the day of sacrifice, and A_{day0} the initially deendothelialized area (n=6 for each conditions). *P<0.05 vs. respective placebo-treated control.

Figure 2. Visualization of the intima of carotid arteries 3 days after endovascular (left) or perivascular (right) injury in ovariectomized mouse.

Top: Representative Evans blue staining of the remaining deendothelialized area in carotids harvested 3 days post-injury. **Middle:** Schematic representation of the intima and media of the injured carotid artery at D3 post-injury. The arrows show the direction of reendothelialization as well as the blood flow. **Bottom (A to E'):** Representative layers of "en face" confocal immunohistochemical analyses. Nuclei appear in blue. A to C': Immunostaining of the intimal tunica against vWF (A and A'), PECAM/CD31 (B and B'), eNOS (C and C'), all three well-recognized markers of endothelial cells. Note the immunostaining of platelet vWF in the not yet reendothelialized area. D and D': Intima tunica BrdU incorporation revealing the proliferating cells (that entered phase S during the last 15 hours). E and E': Media tunica with smooth muscle cell nuclei (oriented transversally). The injured part of the carotid artery is empty of smooth muscle cells in the electric (E'), but not in the endovascular (E) injury model. The sharp limit allow to perfectly define the initial site of the injury, and subsequently to precisely define the "reendothelialized area" (RE), injured intimal area colonized by new endothelium, indicated by the full arrowheads. BrdU incorporation allowed to define a "Regenerative endothelial area" (REGEN), indicated by the empty arrowheads, slightly larger than the RE. This area coincided to decreased expression of vWF and CD31 and increased expression of eNOS.

Figure 3. Effect of E2 on reendothelialization 3 days after perivascular electric injury in ovariectomized mice treated with E2 or placebo (Pl).

A: Representative carotids harvested 3 days after injury and Evans blue staining of the remaining deendothelialized area. Schematic representation of regions of the intima and media of the injured carotid artery. The arrow shows the direction of reendothelialization as well as the blood flow.

B: Intima tunica with immunostaining against eNOS or after BrdU incorporation revealing the proliferating cells (that entered phase S during the last 15 hours).

C: Intima tunica with immunostaining against vWF or CD31.

Nuclei appear in blue. As in Figure 2, the sharp limit allow to perfectly define the initial site of the injury, and subsequently to precisely define the "reendothelialized area" (RE), injured intimal area colonized by new endothelium, indicated by the full arrowheads. BrdU incorporation allowed to define a "Regenerative endothelial area" (REGEN), indicated by the empty arrowheads. REGEN was enlarged by E2 as a consequence of an increase in both the RE and the "retrograde proliferating zone" (RetroP).

Figure 4. Quantification of the effect of E2 on reendothelialization evaluated after perivascular electric injury.

"*En face*" confocal immunohistochemical analysis of the intima tunica allowed the definition and measurement of:

A: the respective length of the "reendothelialized area" (RE), "retrograde proliferating zone" (RetroP) and "regenerative endothelial area" (REGEN)

B: the percentage of BrdU-positive cells, and

C: the total number of cells and BrdU-positive cells in these 3 areas. *P<0.05 vs. respective control.

(n=8 mice in each group)

Figure 5. Effect of E2 on reendothelialization 36 and 50 hours after perivascular electric injury in ovariectomized mice treated with E2 or placebo (Pl).

A: Top: Representative carotids analyzed 36 hours after injury. Nuclei appear in blue. The sharp limit allow to localize the initial site of the injury, and subsequently to precisely define the "reendothelialized area" (RE), injured intimal area colonized by new endothelium, indicated by the full arrowheads. E2 significantly increased EC migration, but the lack of BrdU incorporation revealed that no cells had yet entered S phase. **Bottom:** Quantification of the reendothelialized area (RE) in carotids harvested 36 hours after injury from mice treated or not with E2 (n=7 in each group). Scale bars correspond to 50 μm.

B: Representative carotids analyzed 50 hours after injury. "REGENerative endothelial area" (REGEN), characterized by BrdU incorporation, was detected in E2-, but not yet in placebo-treated mice. Elongated medial smooth muscle cell nuclei are oriented perpendicularly to the blood flow and present only in adjacent uninjured endothelium. Scale bars correspond to 50 μm.

C: Intimal cellular density around the site of injury, 50 h post-injury. The number of propidium iodide-stained nuclei were counted in each 75μm portion, upstream (-) of and downstream (+) from the injury limit. E2 decreased the cell density further in the retrograde uninjured endothelium than did the placebo. Thus, the larger retrograde mobilization of endothelial cells to migrate by E2 accounted for the main increase of cells downstream the injury limit and thus a larger reendothelialized area.

Figure 6. Accentuation of the retrograde proliferation 5 days post-injury in placebo- and E2-treated mice.

A: Representative image of intima tunica 5 days after injury. In order to visualize cells in proliferation, BrdU was injected 15 hours prior to sacrifice. **B:** Quantification confirmed the effect of E2 on RE size. Furthermore, it revealed that RetroP was even further enlarged in both placebo and in E2-treated mice at Day 5 compared to Day 3 and Day 2. *: $P<0.05$ vs. respective placebo; Scale bars correspond to 100 μm.

Figure 1

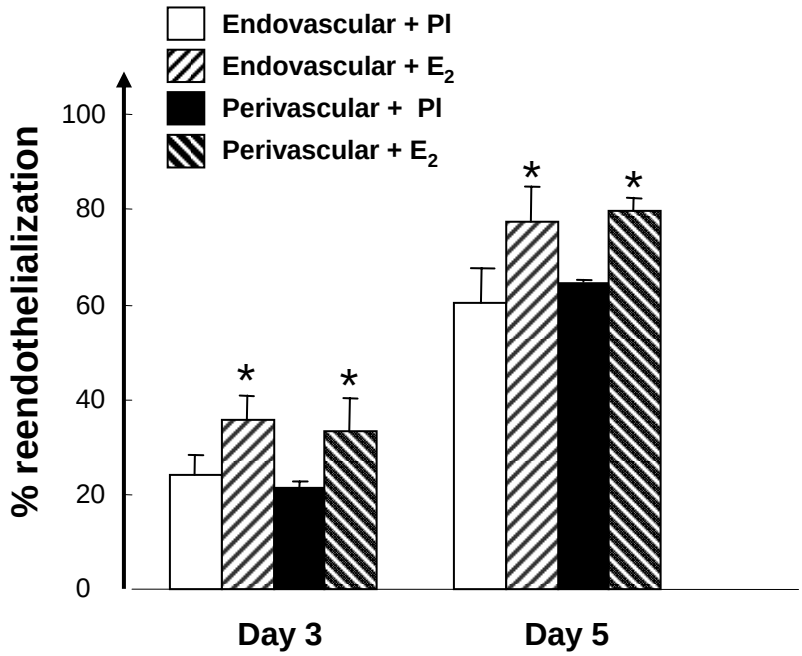
Endovascular + Pl
Endovascular + E2
Perivascular + Pl
Perivascular + E2
% reendothelialization
100
80
60
40
20
0
*
*
*
*
Day 3
Day 5

Figure 2

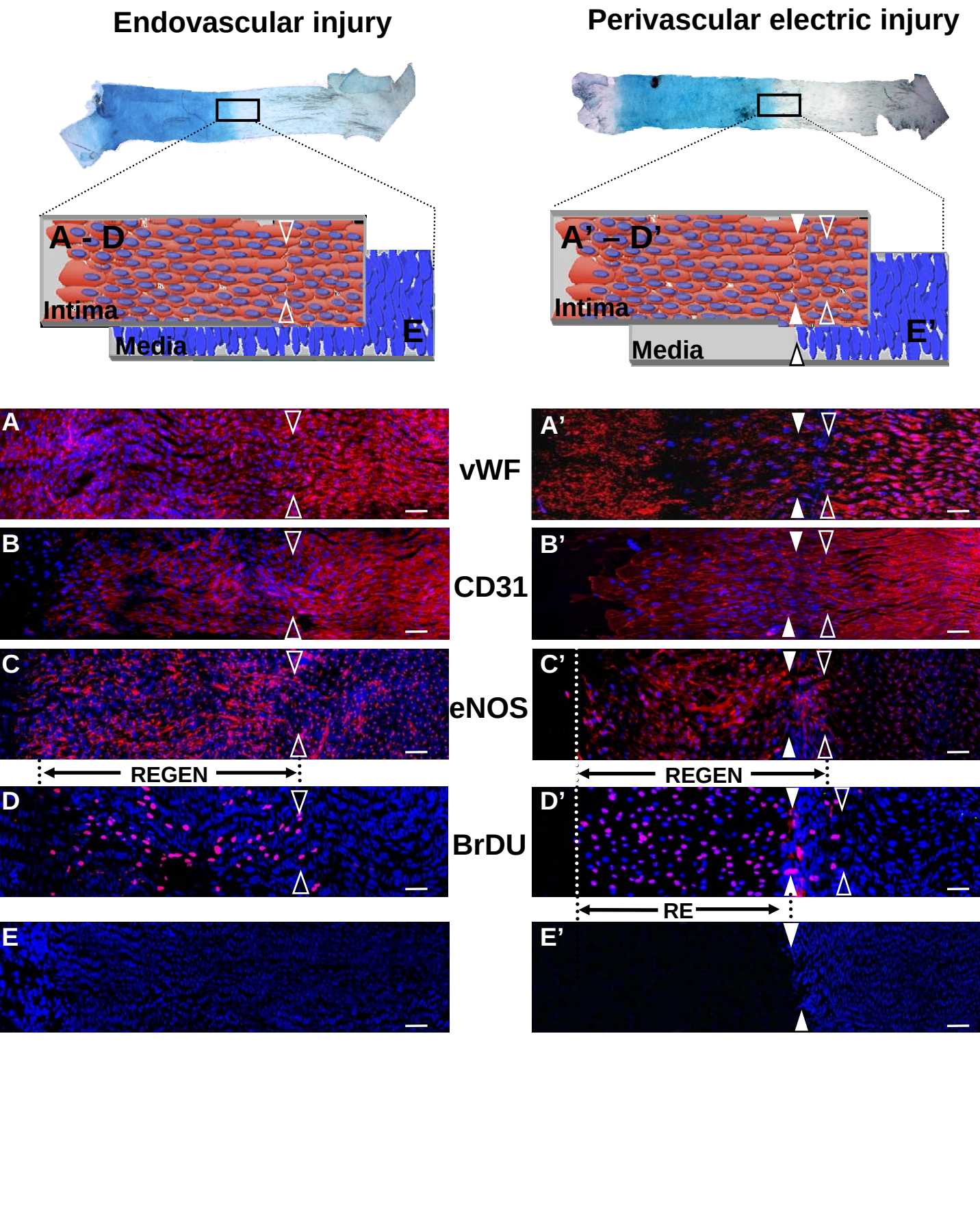
Endovascular injury
Perivascular electric injury
A - D
Intima
Media
E
A’ – D’
Intima
Media
E’
A
A’
vWF
B
B’
CD31
C
C’
eNOS
REGEN
REGEN
D
D’
BrDU
RE
E
E’

Figure 3

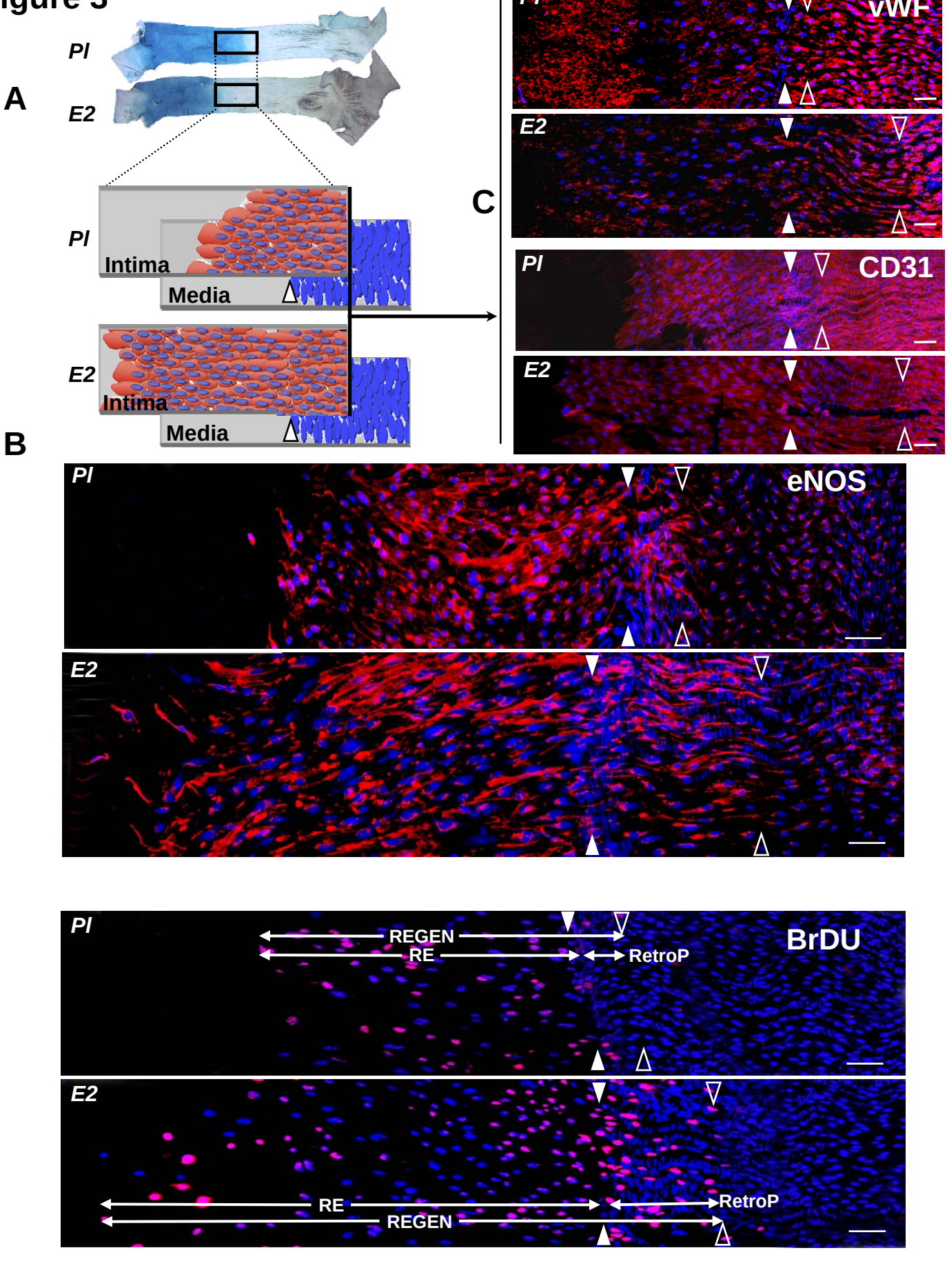
A
PI
E2
B
PI
Intima
Media
E2
Intima
Media
C
PI
vWF
E2
PI
CD31
E2
PI
eNOS
E2
PI
REGEN
RE
RetroP
BrDU
E2
RE
REGEN
RetroP

Figure 4

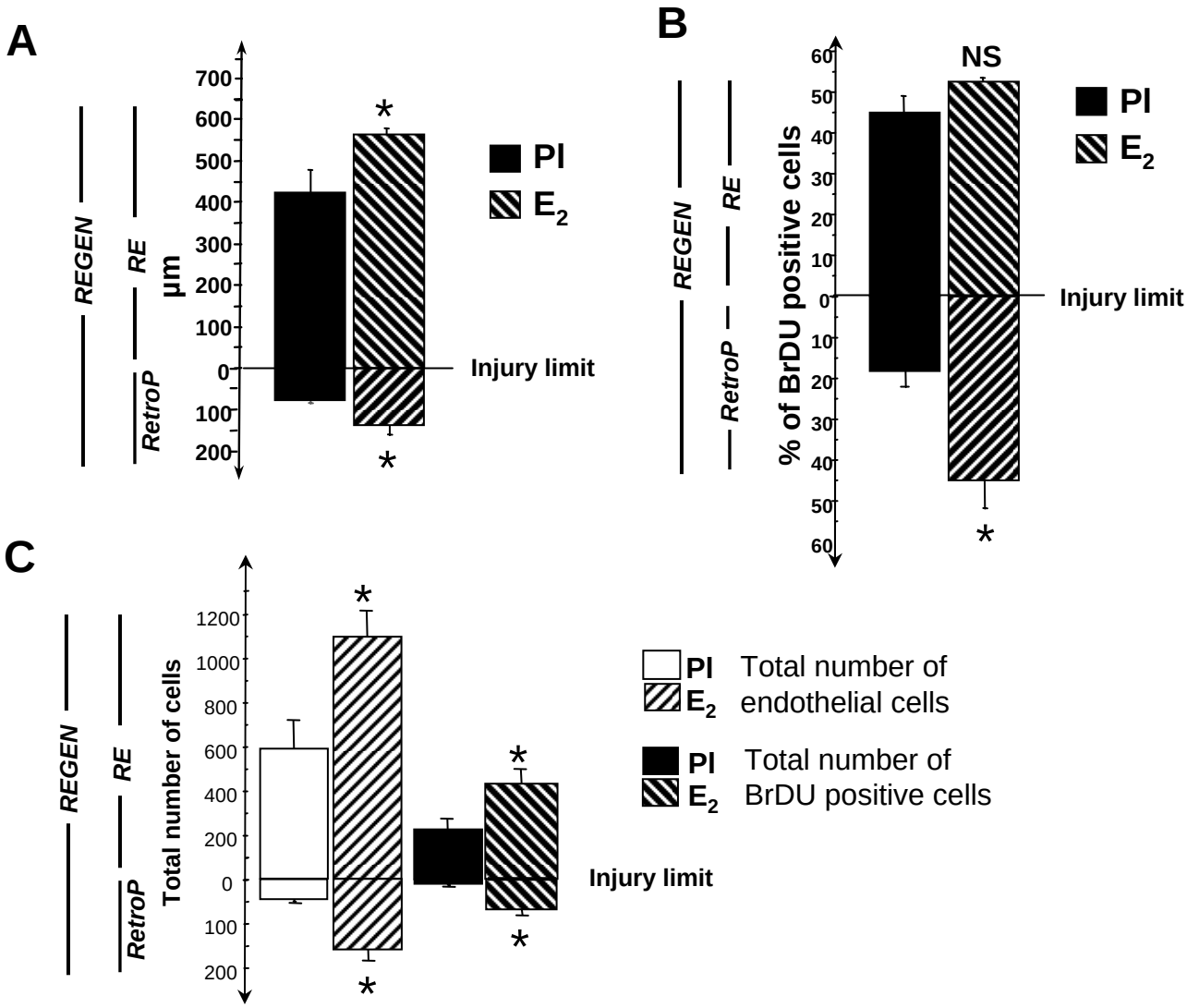
A
REGEN
RE
RetroP
µm
700
600
500
400
300
200
100
0
100
200
Pl
E2
Injury limit
*
*
B
REGEN
RE
RetroP
% of BrDU positive cells
NS
60
50
40
30
20
10
0
10
20
30
40
50
60
Pl
E2
Injury limit
*
C
REGEN
RE
RetroP
Total number of cells
1200
1000
800
600
400
200
0
100
200
Injury limit
Pl Total number of
E2 endothelial cells
Pl Total number of
E2 BrDU positive cells

Figure 5

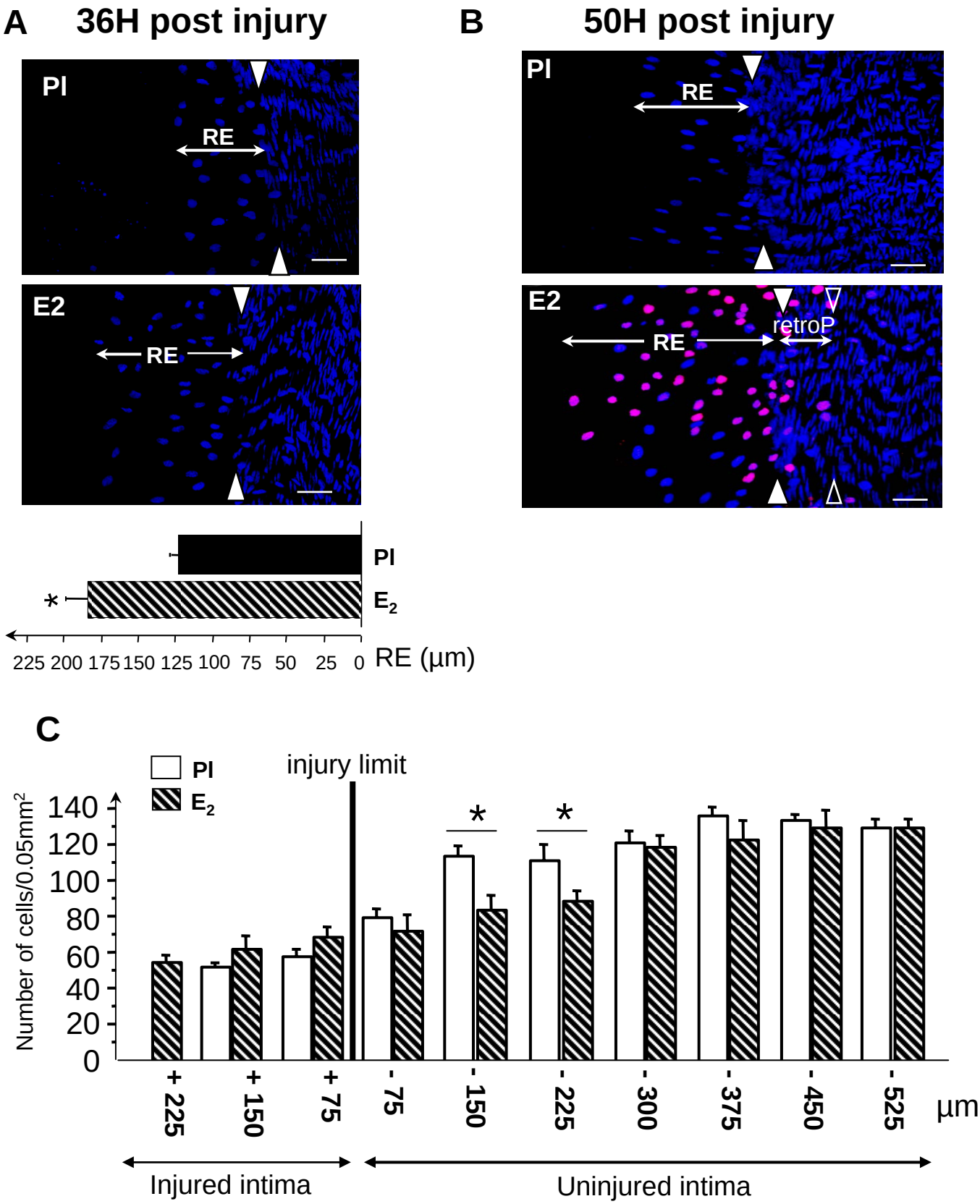
A
36H post injury
PI
RE
E2
RE
B
50H post injury
PI
RE
E2
RE
retroP
PI
E2
*
225 200 175 150 125 100 75 50 25 0
RE (µm)
C
PI
E2
injury limit
Number of cells/0.05mm2
140
120
100
80
60
40
20
0
*
*
+ 225
+ 150
+ 75
- 75
- 150
- 225
- 300
- 375
- 450
- 525
µm
Injured intima
Uninjured intima

Figure 6

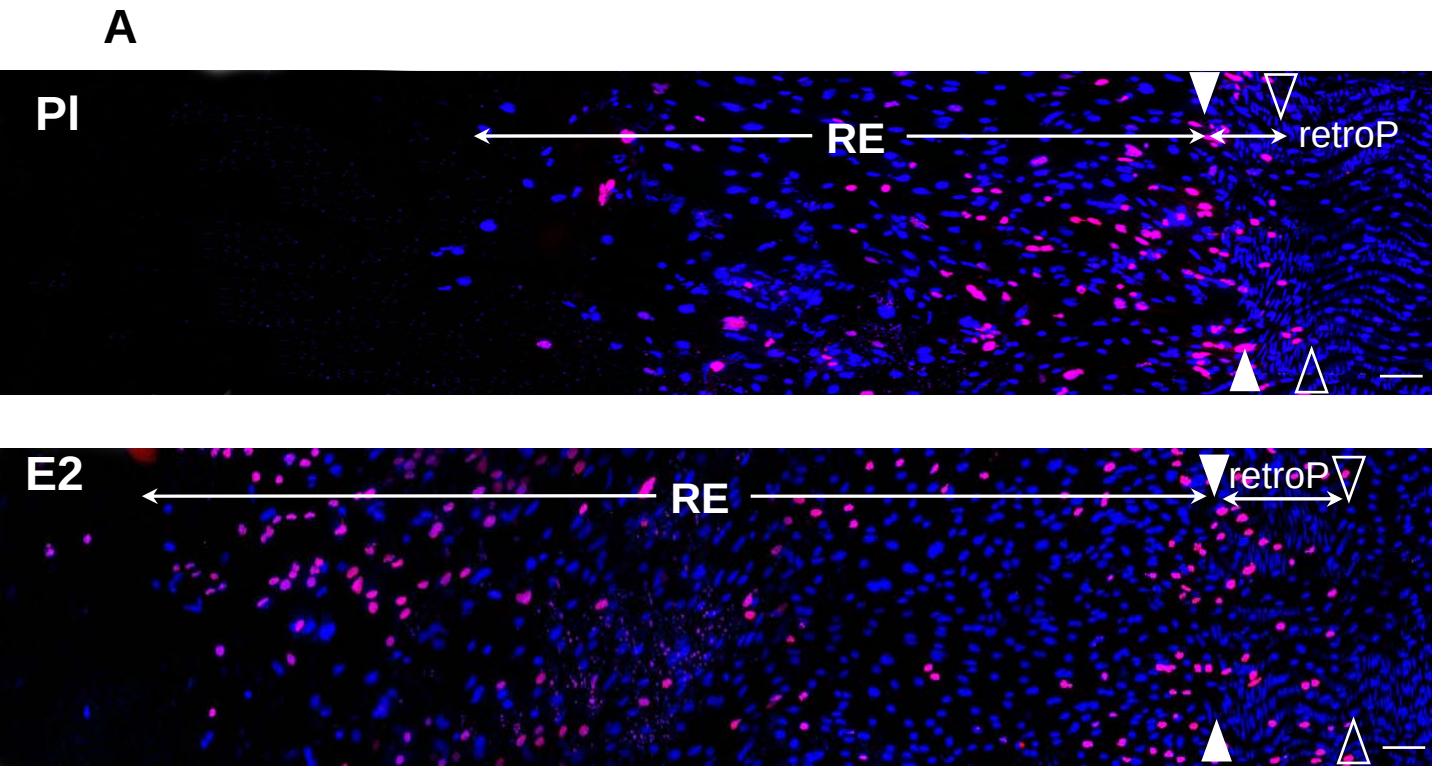
A
PI
RE
retroP
E2
RE
retroP

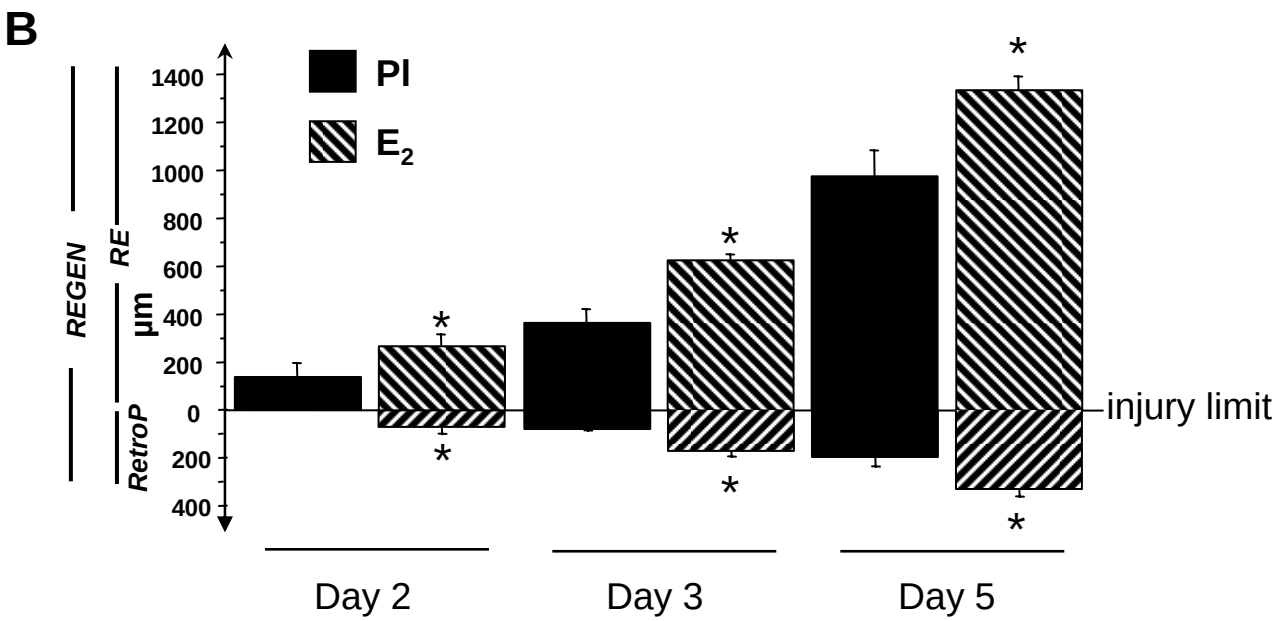
B
PI
E2
1400
1200
1000
800
600
400
200
0
200
400
µm
REGEN
RE
RetroP
injury limit
Day 2
Day 3
Day 5